Modification of TiO_2 Network Structures Using a Polymer Gel Coating Technique

Rachel A. Caruso,*,† Markus Antonietti,† Michael Giersig,‡ Hans-Peter Hentze,† and Jianguang Jia†

Max Planck Institute of Colloids and Interfaces, 14424 Potsdam, Germany, and Hahn Meitner Institute, Glienicker Strasse 100, 14109 Berlin, Germany

Received November 13, 2000. Revised Manuscript Received December 7, 2000

A variety of polymer gels with different chemical composition, architecture, porosity, and surface area have been used as templating materials for the fabrication of porous TiO_2 networks. Titanium isopropoxide was incorporated in the bicontinuous polymer structure where hydrolysis and condensation reactions were carried out, producing a hybrid of polymer and amorphous titania. Calcination of this hybrid resulted in the formation of a continuous, purely inorganic network of either the anatase or rutile crystal phase, with the individual titanium dioxide particles contacting a number of neighbors, thereby forming a continuous three-dimensional structure. The resulting networks have vastly different structures, with porosities as high as 99% and surface areas ranging from 5 to 100 $m^2\ g^{-1}$. These structures may be of importance to various fields of research, including photovoltaics and photocatalysis, because the open "coral-like" network structure of the titanium dioxide allows high access of the titanium dioxide surface to the reaction medium. The potential of the gel coating technology for the construction of more complex chemical systems was illustrated by the assembling of a noble metal/oxide semiconductor hybrid where homogeneously dispersed platinum nanoparticles are integrated within the TiO_2 network. Preliminary studies have shown the titanium dioxide materials to exhibit 75% of the photocatalytic activity of Degussa P25.

Introduction

Templating procedures are widely used in modern materials science to fabricate organic and inorganic structures, regulating their final form and hence their properties. The basis of such methods is the employment of various molecular objects as some type of "mold" to produce a desired product with the required shape and/or interface structure, which is usually obtained as a cast or negative of the original mold. The lyotropic liquid-crystalline phases of amphiphiles,[1−5] block copolymer assemblies,[6] latex particles,[7,8] and electrooxidized alumina[9−12] are some examples of templating materials that have been used to produce porous polymers, metals, mesoporous silicas, and hollow silica spheres. In a previous publication,[13] we demonstrated the novel use of a polymer gel template to produce titanium dioxide networks with high porosity and a continuous network structure. This raised the question of whether this approach may be generalized, i.e., if gels of various chemical compositions and pore sizes can be coated. A related and unanswered question was whether the particle size and the particle connectivity could be controlled by the thickness of the titania coating. Hence, in this work various polymer gels with very different chemical and physical structure will be used to study the effect of template properties on the morphology of the final inorganic network.

The inorganic material chosen for the study of these systems, titanium dioxide, was selected because of its known usefulness in diverse applications. For example, in photocatalysis titanium dioxide has been found to decompose a wide variety of materials in both gas and liquid phases,[14] making it a material beneficial for environmental cleaning and purification processes. Additionally, its durability, stability, and special semiconductor properties make it a frequently studied material

* To whom correspondence should be addressed. Fax: +49 331 567 9502. E-mail: rachel.caruso@mpikg-golm.mpg.de.
† Max Planck Institute of Colloids and Interfaces.
‡ Hahn Meitner Institute.

(1) Göltner, C.; Antonietti, M. *Adv. Mater.* **1997**, *9*, 431−436.
(2) Kresge, C. T.; Leonowicz, M. E.; Roth, W. J.; Vartuli, J. C.; Beck, J. S. *Nature* **1992**, *359*, 710−712.
(3) Beck, J. C.; Vartuli, W. J.; Roth, M. E.; Leonowicz, M. E.; Kresge, C. T.; Schmitt, K. D.; Chu, C. T. W.; Olson, D. H.; Sheppard, E. W.; McCullen, S. B.; Higgins, J. B.; Schlenker, J. L. *J. Am. Chem. Soc.* **1992**, *114*, 10834−10843.
(4) Antonietti, M.; Caruso, R. A.; Göltner, C. G.; Weissenberger, M. C. *Macromolecules* **1999**, *32*, 1383−1389.
(5) Attard, G. S.; Bartlett, P. N.; Coleman, N. R. B.; Elliot, J. M.; Owen, J. R.; Wang, J. H. *Science* **1997**, *278*, 838−840.
(6) (a) Krämer, E.; Förster, S.; Göltner, C.; Antonietti, M. *Langmuir* **1998**, *14*, 2027−2031. (b) Weissenberger, M. C.; Göltner, C. G.; Antonietti, M. *Ber. Bunsen-Ges. Phys. Chem.* **1997**, *101*, 1679−1682.
(7) Caruso, F.; Caruso, R. A.; Möhwald, H. *Science* **1998**, *282*, 1111−1114.
(8) Antonietti, M.; Berton, B.; Göltner, C.; Hentze, H.-P. *Adv. Mater.* **1998**, *10*, 154−159.
(9) Martin, C. R. *Science* **1994**, *266*, 1961−1966.
(10) Hulteen, J. C.; Martin, C. R. *Nanoparticles and Nanostructured Films*; Fendler, J. H., Ed.; Wiley-VCH: New York, 1998; pp 235−262.
(11) Hoyer, P. *Curr. Opin. Colloid Interface Sci.* **1998**, *3*, 160−165.
(12) Foss, C. A., Jr.; Hornyak, G. L.; Stockert, J. A.; Martin, C. R. *J. Phys. Chem.* **1994**, *98*, 2963−2971.
(13) Caruso, R. A.; Giersig, M.; Willig, F.; Antonietti, M. *Langmuir* **1998**, *14*, 6333−6336.

10.1021/cm001222z CCC: $20.00
Published on Web 02/21/2001

in photovoltaics. More recently, a highly amphiphilic titanium dioxide surface[15,16] has led to the development of antifogging and self-cleaning glass and ceramic surfaces. It is expected that a controlled and simple synthesis of a highly porous, high surface area titania will enhance its performance in the assorted applications in which it is currently used.

Mesostructures of titanium dioxide have been produced using alumina membranes,[17−19] latex particles,[20,21] and monodisperse emulsions[22] as templates. The alumina membranes (of thickness 10−100 μm) with hexagonally packed cylindrical pores of uniform diameter (ranging from 5 to 200 nm), and pore densities of up to 10^{11} pores cm^{-2}, are produced by the anodization of aluminum metal in acidic solution.[10] Hoyer[17] used a two-step templating process involving the production of a poly(methyl methacrylate) negative of the porous alumina membrane, on which electrochemical deposition of amorphous titania was performed. Upon heating to 450 °C, nanotubes of TiO_2 in the anatase form, with a wall thickness of about 25 nm and inner diameters of between 50 and 70 nm, were produced. Martin et al.[19] used a sol−gel chemistry based one-step process within alumina pores of either 200 or 22 nm diameter to form either TiO_2 tubules or fibrils, depending on the immersion time of the alumina membrane in the sol solution. The alumina template was removed after heating by dissolution in aqueous NaOH. A calculated surface area of 5.1 $m^2\ g^{-1}$ was reported for the 200 nm diameter anatase fibrils.

Methods involving the use of ordered, dried latex particles for the creation of macroporous networks of TiO_2 have recently been reported.[20,21] Holland et al.[20] obtained a Brunauer−Emmett−Teller (BET) surface area of 22 $m^2\ g^{-1}$ for their anatase TiO_2 sample containing close-packed, open-pore structures with 320−360 nm voids. Wijnhoven and Vos[21] produced air spheres, with radii between 120 and 1000 nm within the titania material, with a calculated TiO_2 density between 12 and 20 vol %. Another controlled TiO_2 lattice was formed using emulsion templating.[22] Because of the vigorous reaction of the titanium precursor with water, the emulsion was formed by stabilizing oil droplets in a formamide solution using a polymeric surfactant. Again highly uniform, spherical pores with sizes in the 50 nm to 10 μm range, and lattice porosities of up to ~90%, were produced. Without the use of templating materials, the sol−gel process can produce high surface area titanium dioxide materials (250 $m^2\ g^{-1}$);[23] however, the porosity of such a material is not as high (<57%) as that obtained in the above-mentioned template processes.

The controlled fabrication of highly porous TiO_2 networks with high surface area by templating polymer gels adds a new dimension to the existing collection of template processes in that the final structure is more variable; the pores in TiO_2 are not limited to cylindrical or spherical form. There is more flexibility in the initial polymer shape and structure; therefore, the pore sizes can be altered, as can the porosity and surface area of the final material. This is especially beneficial when high absolute porosity and high surface area are to be combined, because it is necessary for improved contact between a solid titania catalyst and a reactant gas or liquid. The gel template is also conveniently removed during the calcination step in which the amorphous titania crystallizes. The resulting inorganic network is monolithic in nature; i.e., it is a uniform piece that retains its shape and does not crack or crumble to a powder during the heating stage, thus making a three-dimensional material of controlled outer dimensions that can be handled and fixed for application purposes. The potential of the gel coating technique was shown with the synthesis of the so-called "coral-like" TiO_2.[13]

The mesostructured gels, which are from the perspective of pore connectivity most promising for templating, are in fact products of a template process themselves. These gels are made in the presence of structure-directing amphiphiles or amphiphilic polymers,[4] and although this process does not result in a direct cast of the original surfactant structure, it allows a great variety of architecture of the intermediary polymeric framework. The use of different template directors and different combinations of monomer, surfactant, and water can easily alter the properties of the polymer gels,[4,24] and therefore the resulting inorganic network is expected to be modified.

Another advantage of the gel coating technique is that sequences of coating procedures can be employed, resulting in materials that are layered on the nanometer scale and materials with potentially very different electronic or optical properties. This is somewhat reminiscent of modern chemical vapor deposition technologies for the fabrication of functional surfaces and circuits. If a first layer is not continuous in itself but deposited as single particles onto the gel, a second continuous layer is expected to enclose the previously deposited particles. This is shown schematically in Figure 1.

This possibility will be demonstrated here by performing a sequence of reactions where a platinum salt is bound onto the polymer network and reduced to form platinum nanoparticles. This compound material is coated with the titanium precursor. As the final product, we expect a mesostructured TiO_2 network that is functionalized by the incorporation of well-defined Pt nanoparticles. Such a functionalization is also interesting from the application point of view, because metal

(14) For example, see: (a) Ohko, Y.; Tryk, D. A.; Hashimoto, K.; Fujishima, A. *J. Phys. Chem. B* **1998**, *102*, 2699−2704. (b) Sadeghi, M.; Liu, W.; Zhang, T. G.; Stavropoulos, P.; Levy, B. *J. Phys. Chem.* **1996**, *100*, 19466−19474. (c) Sun, L. Z.; Bolton, J. R. *J. Phys. Chem.* **1996**, *100*, 4127−4134. (d) Choi, W. Y.; Hoffmann, M. R. *Environ. Sci. Technol.* **1997**, *31*, 89−95.

(15) Chikuni, M.; Kojima, E.; Kitamura, A.; Shimohigoshi, M.; Watanabe, T. *Nature* **1997**, *388*, 431−432.

(16) Wang, R.; Hashimoto, K.; Fujishima, A.; Chikuni, M.; Kojima, E.; Kitamura, A.; Shimohigoshi, M.; Watanabe, T. *Adv. Mater.* **1998**, *10*, 135−138.

(17) Hoyer, P. *Langmuir* **1996**, *12*, 1411−1413.

(18) Hoyer, P. *Adv. Mater.* **1996**, *8*, 857−859.

(19) Lakshmi, B. B.; Dorhout, P. K.; Martin, C. R. *Chem. Mater.* **1997**, *9*, 857−862.

(20) Holland, B. T.; Blanford, C. F.; Stein, A. *Science* **1998**, *281*, 538−540.

(21) Wijnhoven, J. E. G.; Vos, W. L. *Science* **1998**, *281*, 802−804.

(22) Imhof, A.; Pine, D. J. *Adv. Mater.* **1998**, *10*, 697−700.

(23) Bischoff, B. L.; Anderson, M. A. *Chem. Mater.* **1995**, *7*, 1772−1778.

(24) Hentze, H.-P.; Krämer, E.; Berton, B.; Förster, S.; Antonietti, M.; Dreja, M. *Macromolecules* **1999**, *32* (18), 5803−5809.

Table 1. Polymer Gel Composition

polymer gel	mass (g) template director (amphiphile)	H_2O	monomer 1	monomer 2	cross-linker	initiator (KPS)
B561	0.500 (B56)	3.000	1.300 (DMA)		0.200 (MBA)	0.050
B562	1.200 (B56)	3.000	1.300 (DMA)		0.200 (MBA)	0.050
T601	2.000 (T60)	4.000	0.500 (AA)	0.500 (GMA)	0.100 (EGDMA)	0.060
B581	1.000 (B58)	8.000	1.000 (AA)	1.000 (GMA)	0.200 (EGDMA)	0.050
B582	1.000 (B58)	8.000	1.000 (AA)	1.000 (GMA)	0.400 (EGDMA)	0.050
CTA1	0.650 (CTAB)	3.607	0.372 (A)	0.346 (S)	0.026 (*m*-DIB)	0.020[a]
CTA2	0.514 (CTAB)	3.900	0.294 (A)	0.273 (S)	0.021 (*m*-DIB)	0.020[a]
SE1	2.400 (SE30/30)	4.800	0.250 (AA)	0.250 (GMA)	0.100 (EGDMA)	0.050
SE2	3.000 (SE30/30)	4.500	0.234	0.234	0.094 (EGDMA)	0.050
EK1−3	PEO/PB, hexagonal packing					γ-radiation

[a] AIBN.

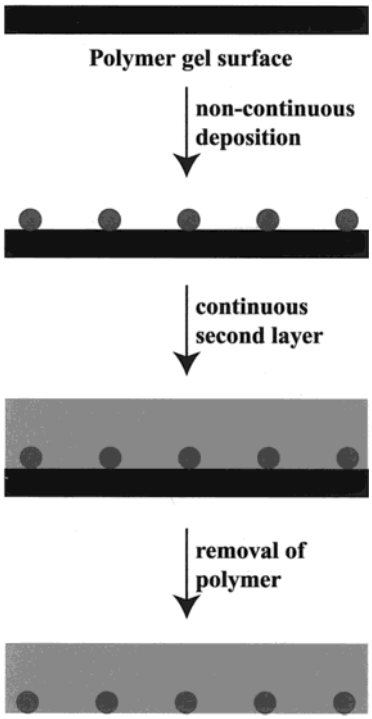

Figure 1. Schematic illustrating the gel coating technique used in sequence. Initially a noncontinuous first layer of nanoparticles, for example, is deposited onto the polymer gel surface. This is followed by deposition of a second continuous layer and then removal of the polymer template by heating to yield the desired composite material.

colloids within titanium dioxide networks have been shown to influence the properties of the semiconductor,[25] such as their effectiveness in electron−hole separation.

Experimental Section

Materials. To synthesize inorganic networks with different architectures and to determine possible limits of the gel coating technique, a variety of polymer gels with varying pore sizes, morphologies, and chemical compositions were produced by variation of both the template director and monomer. The template directors utilized for porous polymer production include the surfactants Brij 56 (B56; main component decaethylene glycol hexadecyl ether) and Brij 58 (B58; main component eicosaethylene glycol hexadecyl ether), both obtained from Fluka Chemika. Cetyltrimethylammonium bromide (CTAB) and Tween 60 [T60; polyoxyethylene (20) sorbitan monostearate] were obtained from Aldrich. A block copolymer from Goldschmidt AG [SE30/30, containing polystyrene-*b*-poly(ethylene oxide) with a block length of 3000 g mol^{-1}] was also used as a template for the formation of a polymer gel. The monomers employed in these experiments [acrylic acid (A), acrylamide (AA), glycidyl methacrylate (GMA), *N*,*N*-dimethylacrylamide (DMA), and styrene (S)] were all purchased from Aldrich. *N*,*N*'-Methylenebis(acrylamide) (MBA), *m*-diisopropenylbenzene (*m*-DIB), and ethylene glycol dimethacrylate (EGDMA), all Aldrich products, were used as cross-linkers and 2,2'-azobis(isobutyronitrile) (AIBN; Fluka Chemika) and potassium persulfate (KPS; Aldrich) as initiators. The titanium precursor titanium(IV) isopropoxide (99.999%) and 2-propanol (99.5%) were from Aldrich. The platinum salt hydrogen hexachloroplatinate(IV) hydrate, used to produce colloidal platinum particles within the polymer gel and salicylic acid, for the photodecomposition reactions, were also Aldrich products.

Polymer Gel Formation. The surfactant and block copolymer template directors were combined with water under gentle agitation before the monomer(s) and cross-linker were added. Agitation continued until homogeneous solutions were obtained. Following the addition of the initiator, the test tube containing the mixture was placed in an oil bath at 55 °C for a period of 5−24 h, depending on the system, while polymerization occurred. Table 1 lists the template directors, compositions, and abbreviations of the polymers discussed in this paper.

TiO_2 Network Fabrication. The removal of water present within the gels was required because the titanium precursor rapidly undergoes hydrolysis in the presence of H_2O. Therefore, a solvent exchange process, involving a gradual increase in the amount of ethanol to water and then propanol to ethanol, was used to transfer the polymer gels from water into 2-propanol. This method excludes water from the polymer gel and also decreases the possibility of structural damage to the gel due to rapid change of the solvent. Once this had been achieved, the gels could be placed into a neat titanium(IV) isopropoxide solution for precursor permeation for a period of 6 h. The precursor-soaked gel was then placed into a 2-propanol/H_2O mixture (1:1 by volume) for 6 h, during which time hydrolysis and condensation occurred. After drying, the polymer gels containing amorphous titania were calcined to temperatures of either 450 or 990 °C, which resulted in pyrolysis of the polymer and crystallization of the titania to produce either anatase or rutile phase TiO_2 colloidal structures, respectively.

Incorporation of Platinum Nanoparticles. The reduction of metal salts to produce colloidal particles bound to polymers and gels can be carried out in numerous ways.[26] The method found to work most successfully for the polymer gel chosen was that of reduction by refluxing in alcohol. The polymer gel was soaked in an aqueous hexachloroplatinate solution (0.05 M) for a period of 3 days. During this time the

(25) Linsebigler, A. L.; Lu, G.; Yates, J. T., Jr. *Chem. Rev.* **1995**, *95*, 735−758.

(26) Mayer, A.; Antonietti, M. *Colloid Polym. Sci.* **1998**, *276*, 769−779.

polymer gel became yellow throughout, which is due to coordinative and/or Coulombic binding of the metal precursor to the functional polymer gel. The solvent was slowly exchanged to ethanol, and the solution (50 mL) was bubbled with argon before boiling under reflux for a period of 6 h, during which time the ethanol solution became gray and the polymer gels changed from light yellow to a darker yellow with a black outer surface. Further solvent exchange to 2-propanol prepared the gels for titanium precursor incorporation.

Characterization. A critical point dryer, CPD 030 from BAL-TEC, was used to dry the gels after solvent exchange from water to ethanol and then to acetone (a method known to suppress drying artifacts[27]). To examine both the original gel structure and that of the resulting TiO_2 network, the dried or calcined systems were broken to expose fresh surfaces and mounted onto carbon-coated stubs before sputter coating for scanning electron microscopy (SEM; Zeiss DSM 940 instrument) investigation. Ultrathin sections of the network (30−100 nm in thickness) were obtained using a Leica ultracut UCT ultramicrotome after setting the sample in an LR-White resin. The thin sections were placed onto either carbon or noncoated copper grids. A Philips CM12 high-resolution transmission electron microscope (HRTEM) equipped with an EDAX 9800 analyzer was employed for analysis of the finer details of the local structure. To determine the temperatures of total polymer pyrolysis and the weight percent of polymer to TiO_2 in the intermediate stages, a Netzsch TG 209 apparatus was used for thermogravimetric analysis. The specific surface area was obtained from BET analysis after N_2 sorption using a Micromeritics Gemini II 2375 surface area analyzer. Wide-angle X-ray scattering (WAXS), Enraf-Nonius PDS-120, was used to confirm crystal structures observed during HRTEM analysis.

Salicylic Acid Photodecomposition. The decomposition of salicylic acid was used to test the ability of the titanium dioxide networks produced to perform photocatalytic reactions. A stirred aqueous solution (6 mL) of salicylic acid (2.9×10^{-4} M) containing the titanium dioxide sample (0.015 g) was illuminated with a Marva 100 W, high-pressure mercury lamp (HBO 101/2). A cutoff filter (WG-320, Schott) was used to remove the short-wavelength light during illumination. The absorbance spectra of the salicylic acid solutions were monitored as a function of illumination time with an Agilent 8453 UV−vis spectrometer. The photocatalytic properties of a standard titanium dioxide sample, Degussa P25, were also monitored under the same conditions for comparison.

Results

Polymer Gels. The synthesis of porous polymer gels using surfactant phases as template directors follows the recipes described in the literature.[4,28] The hydrophilic monomer is found in the aqueous domains and during polymerization and network construction is limited to these areas. Because of disturbance of the phases during polymerization, the resulting polymer gel is not a direct cast of the original phase structure. The control of the network topology is more due to demixing and the anisotropy of transport processes throughout the reaction.[4] The SEM images of a selection of the polymer gels used in this study are shown in Figure 2.

The gels are homogeneous and porous in structure. Distinct differences resulting from the different materials used during the gel formation are discernible. Globular gels are the outcome of the combination of an aqueous B56 solution and DMA monomer (see Figure 2a for an example). Although both of the gels from the B56/DMA series have similar features, the gel produced using less surfactant has smaller dimensions; i.e., the polymer globules are smaller, as are the pore sizes, than the gels resulting when a higher concentration of surfactant is used. The copolymer gels in Figure 2b,c are not globular but exhibit a flatter structure, with thin interconnecting fibers. These features are especially evident in the cases of the B581 (Figure 2b) and B582 (not shown) gels. The difference in structure observed for the B581 and B582 gels, where the difference in composition is the quantity of the cross-linker, is a more compact arrangement for the more tightly cross-linked gel B582. The pores are somewhat smaller and the polymer structure finer, but more dense. When using the aqueous T60 system as the template director, a more tightly packed polymer with smaller pore sizes eventuates (Figure 2c). The SE1 and SE2, CTA1 and CTA2, and EK1−3 gels have even smaller pores that are difficult to distinguish at this magnification on the SEM. Figure 2d shows an example of the SE1 gel.

The polymer gels are white to transparent in appearance when swollen with water or alcohol and are generally stable enough to be cut with a blade and transported from solutions with tweezers. CTA2 is the only exception to this in that it is jellylike, and therefore extra care is required in its handling so as not to tear the polymer. Both CTA1 and CTA2 swell and shrink significantly in alcohol and water, respectively, which underlines that their mesoscopic topology is not closed. On the whole, the change in size of the other polymer gels when in different solvents is not significant, indicating, highly cross-linked polymer scaffolds.

The porosity and structure of the gels vary with different monomer, surfactant, and water quantities. The porosity of the wet gels can be calculated from the known primary composition used during polymer formation. These values are listed in Table 2. The specific surface areas of the dried gels measured using N_2 adsorption are also noted in this table.

For further calculations, it is necessary to know the relative amount of titania bound to the gel. The binding is definitely incomplete, because the water/alcohol solution in which the precursor swollen gel was placed for hydrolysis became cloudy because of precursor or hydrolyzed titania leaching from the gel and going into solution. For most of the gels, we estimate that the amount of nonspecifically hydrolyzed titania is minor, i.e., below 10%. On drying, the titania-filled gels were either white or yellow.

TiO_2 Networks. The TiO_2 networks are yellowish immediately after calcination but soon after become white. Generally, the remaining titanium dioxide structure retains the shape of the initial polymer/titania system, with only slight shrinkage. The CTA1 and CTA2 gels are not coherent enough to produce TiO_2 networks, and smaller pieces, but not powders, are obtained. The networks can be handled with tweezers, although applying too much force does result in damage. A chalky substance best describes the final TiO_2 product. Figure 3 shows SEM images, on the same scale as Figure 2, of the resulting TiO_2 networks. Again, homogeneous, porous structures are observed. The individual colloidal

(27) Reimer, L.; Pfefferkorn, G. *Scanning Electron Microscopy*; Springer: Berlin, 1972.

(28) (a) Chieng, T. H.; Gan, L. M.; Chew, C. H.; Ng, S. C.; Pey, K. L. *J. Appl. Polym. Sci.* **1996**, *60*, 1561−1568. (b) Antonietti, M.; Hentze, H.-P. *Colloid Polym. Sci.* **1996**, *274*, 696−702. (c) Antonietti, M.; Hentze, H.-P. *Adv. Mater.* **1996**, *8*, 840−844.

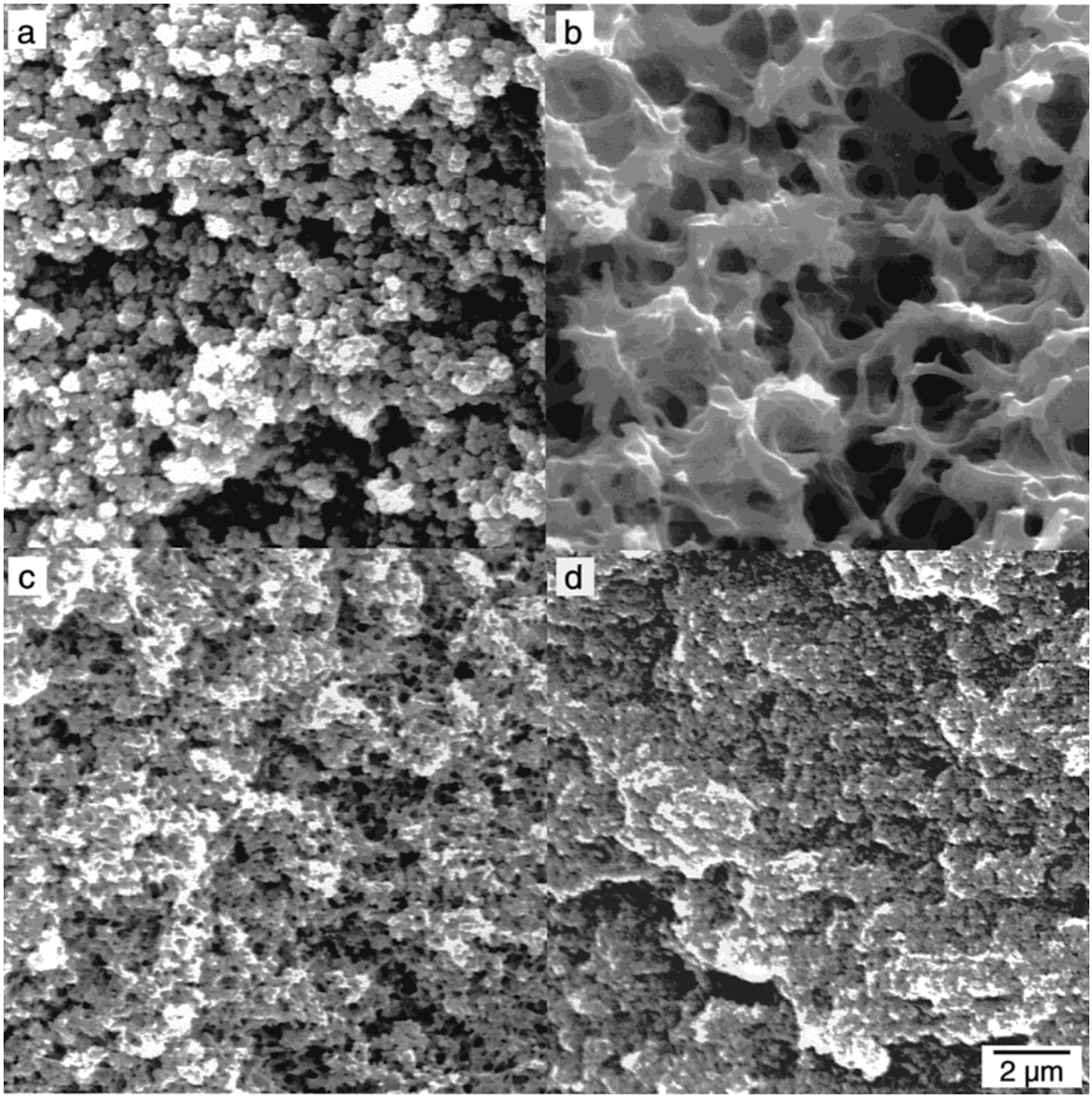

Figure 2. SEM images of the critical point dried polymer gels. (a) B562, (b) B581, (c) T601, and (d) SE1 polymer gels show homogeneous pores with the pore size ranging from micrometers down to tens of nanometers in diameter.

Table 2. Polymer Gel Properties

polymer gel	calcd porosity (vol %)	specific surface area ($m^2\ g^{-1}$)
B561	69	18
B562	73	19
T601	84	27
B581	80	7.3
B582	79	9.8
CTA1	85	42
CTA2	88	54
SE1	91	29
SE2	92	38
EK1−3		*a*

[a] Surface area not measurable because gel requires solvent to swell pores.

particles making up these arrangements cannot be distinguished in the SEM micrographs (the particles can be seen in TEM micrographs; see later). These titania networks are produced on a much shorter time scale (days versus weeks) than the spongelike structures recently obtained by infiltrating titania nanoparticles within similar polymer gel structures.[29]

Comparison of the polymer gel structures in Figure 2 with the inorganic network structures in Figure 3 shows a strong correlation. Although a direct copying is not achieved, it is seen that both the main architecture and the correlation lengths are preserved. The titanium dioxide resulting from the B561 and B562 gels (see Figure 3a for an example) is globular, similar to the initial gel. The diameters of the TiO_2 globules are somewhat smaller than that of the polymer gel, which is presumably due to a slight shrinkage during the heating stage. The networks obtained in the B581 (Figure 3b) and B582 systems clearly show direct plating or coating of the polymer, producing pore sizes similar to those of the polymer gel, and the hollow tubes in the network give evidence of the presence of the polymer fibers. For the T601 system, shown in Figure 3c, the outcome is a more compact structure compared

(29) Breulmann, M.; Davis, S. A.; Mann, S.; Hentze, H.-P.; Antonietti, M. *Adv. Mater.* **2000**, *12*, 502−507.

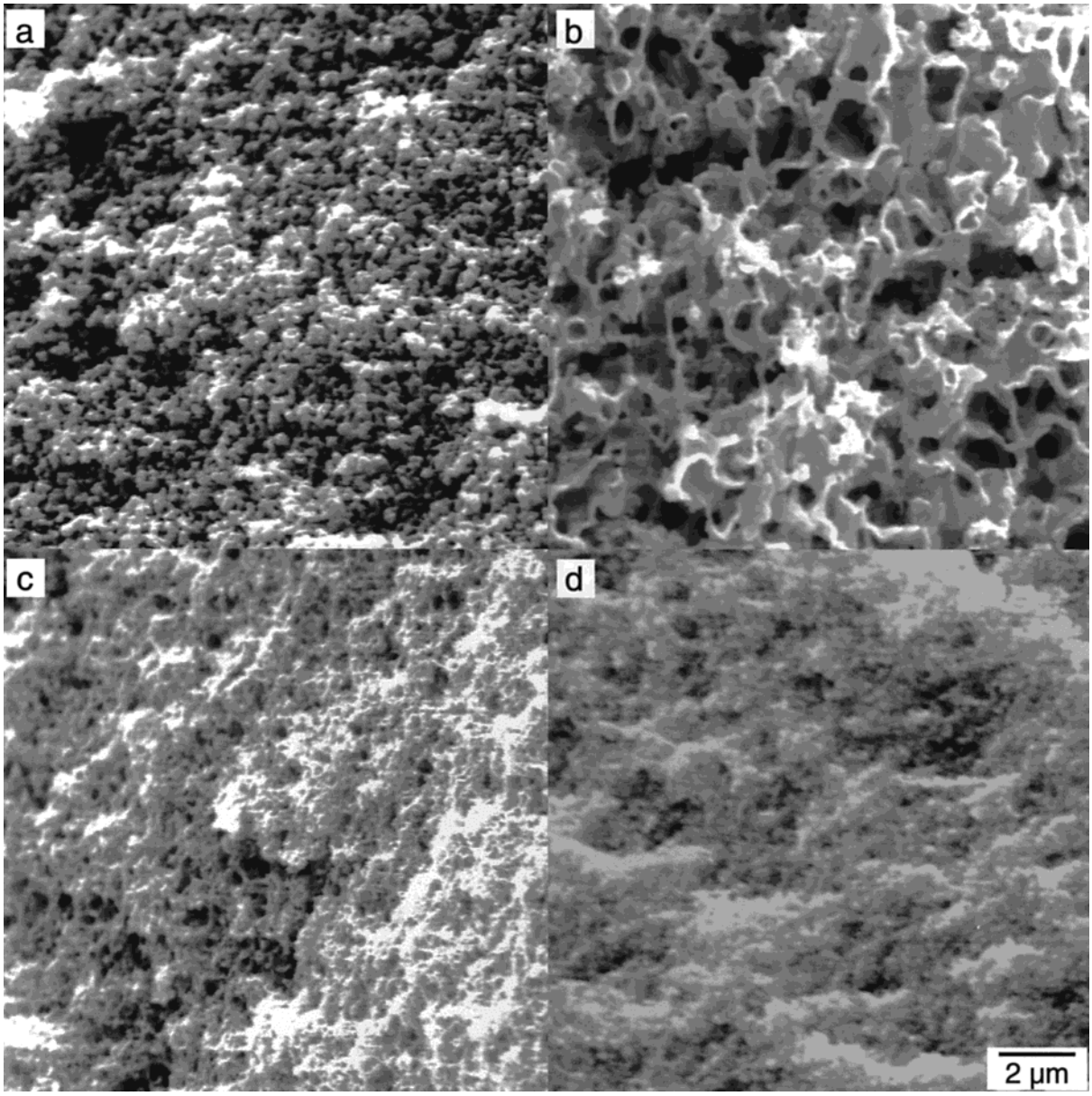

Figure 3. SEM images of the TiO_2 networks with homogeneous pores resulting from the incorporation of titania into the following polymer gels: (a) B562, (b) B581, (c) T601, and (d) SE1.

to the previously described networks. It is again difficult to distinguish pores from the structures resulting after calcining of the CTA1, CTA2, SE1, SE2, and EK1−3 systems using SEM (for an example, see Figure 3d, which shows the TiO_2 network resulting from templating of the SE1 polymer gel), due to the small pore sizes involved.

To obtain information about the characteristics of the smaller pore systems, the polymer gels and the eventuating titanium dioxide entities were set in resin and ultramicrotomed into very thin slices (30−100 nm). The ultrathin sections of the samples were analyzed using TEM. A selection of these is displayed in Figure 4.

Typical for the TiO_2 networks with larger pores, TEM images of the ultrathin sections display a rather tight, single strand of primary TiO_2 colloids, for example, samples B581 and B582, where continuous chains of TiO_2 colloids are observed (Figure 4a,b). In the ultramicrotomed sample, the pore is visible as a ring of particles, the size of which varies between 200 nm and micrometers. The visibility of the pores decreases for the networks with finer pores, which is partly due to the fact that the ultramicrotomed sample contains more than one layer of particles. Hence, the systems were thinned to about 5 nm using ion milling prior to the TEM investigation. For the gels CTA1 and CTA2, SE1 and SE2, and EK1−3, the primary TiO_2 particles are found in loosely connected patches (Figure 4c,d). This low connectivity of the particles is undesirable, because it is connected with a lower mechanical performance and a lower electrical conductivity. The reason for this difference in particle connectivity between large and small pore networks is, to our understanding, closely related to the crystallization mechanism which transfers the previously amorphous titania to the arrangements of crystals. Because the gels are soaked in the same amount of titania precursor, a polymer gel with high surface area is coated with a thinner layer of titania than a system with wide pores. If this layer thickness is below the average size of the formed crystals, the

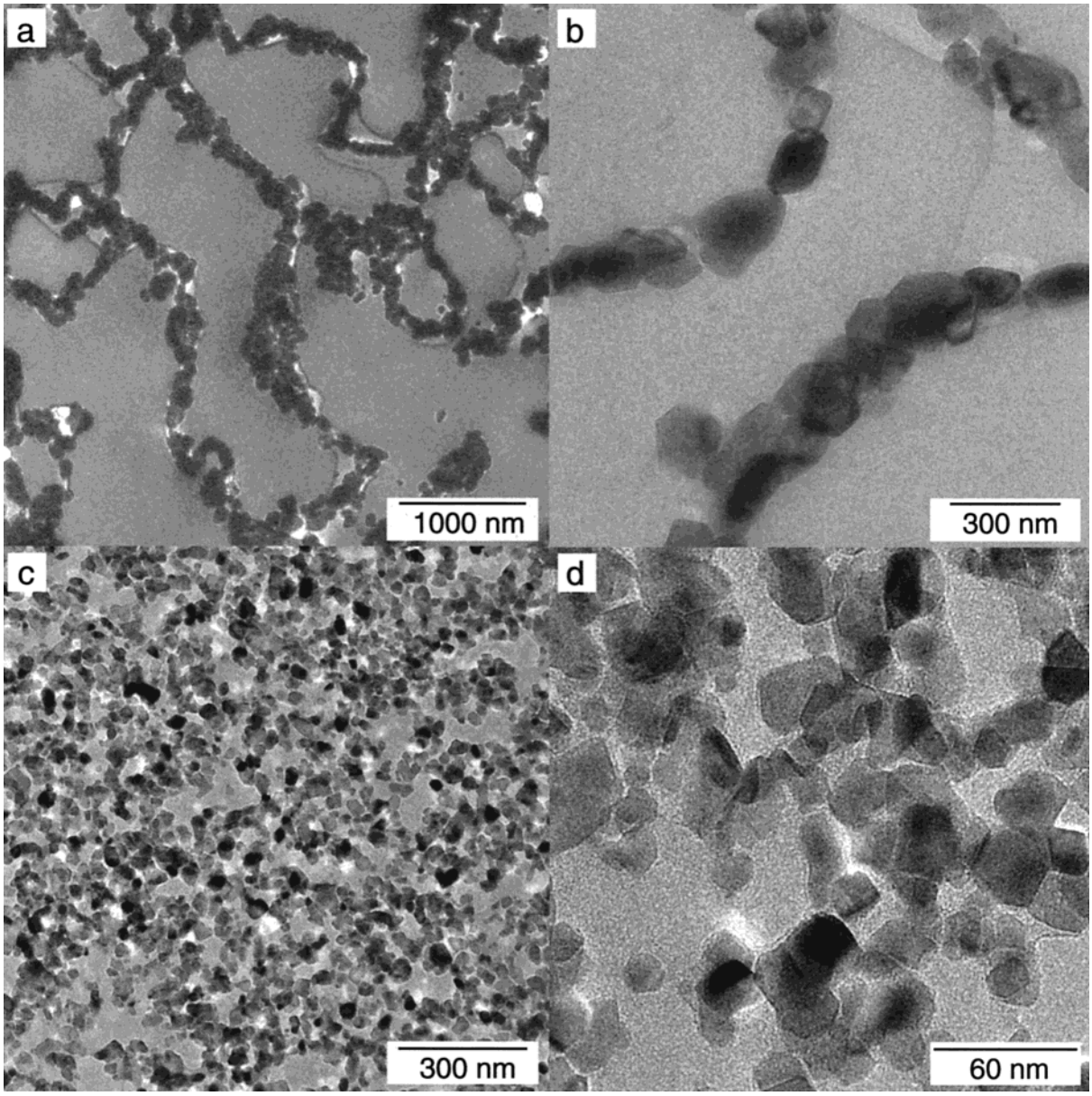

Figure 4. TEM images of an ultramicrotomed TiO_2 network resulting from the B581 polymer gel (a and b) and an ion-milled TiO_2 network from the EK1 gel (c and d). The interconnected TiO_2 colloids can be clearly seen in these images.

crystals cannot interconnect and clusterlike arrangements are generated. It is seen in Figure 4a−d that the crystal size somewhat depends on the layer thickness but does not compensate the full effect. Cohesive crystalline layers with structural details on the scale below 100 nm made by the gel coating technique, therefore, rely on the presence of nanocrystals smaller than those obtained by the present reaction conditions. As a matter of principle, better layers can only be made under optimized nucleation conditions or with a better nucleating material. This will be the subject of a forthcoming paper.

The networks heated to 450 °C consisted of the anatase phase of titanium dioxide. This could be observed using HRTEM, electron diffraction, or WAXS after grinding the sample (as shown in Figure 5). As described earlier,[13] a pure rutile phase can also be obtained by increasing the temperature at which calcination is conducted. Carbon was not detected during energy-dispersive X-ray analysis of the calcined sample.

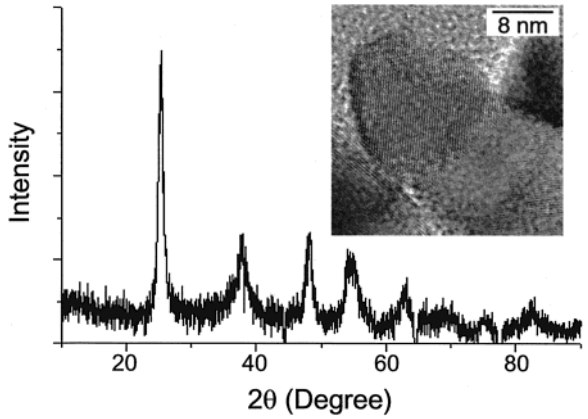

Figure 5. WAXS results from a ground sample, indicating that the total network is in the anatase phase. The inset displays a HRTEM image of the TiO_2 crystals, showing lattice plane spacing of 0.352 nm, corresponding to the anatase phase.

Various parameters, including the calculated porosity, specific surface area, and pore and colloid diameters,

Table 3. TiO_2 Network Properties

polymer gel template	calcd porosity (vol %)	wt % remaining[a]	specific surface area[b] ($m^2\ g^{-1}$)	pore diameter range[c,d] (nm)	TiO_2 colloid diameter range[c] (nm)
B561	98	21.5	20	70−900	25−175
B562	97	28	11	100−3000	15−165
T601	99	26	39	10−325	5−40
B581	98	25	4.9	200−3000	25−175
B582	98	29.5	9.3	25−2300	20−110
CTA1	94	44	62	5−60	5−30
CTA2	94	68	76		
SE1	99	39	49	3−37	10−40
SE2	99	44	59	5−20	7−20
EK1		15	99	2−100	4−14
EK2		12	54	5−175	7−50
EK3		13	82	3−24	8−45

[a] TGA. [b] BET. [c] TEM. [d] SEM.

of the studied TiO_2 networks are listed in Table 3. The porosity was calculated from the reaction parameters; i.e., the relative remaining weight of the sample after polymer pyrolysis was divided by the titania density and compared with the total reaction volume. Sorption measurements were used to calculate the specific surface area using the BET method. The pore diameters were measured from SEM and TEM micrographs and the colloidal dimensions from TEM micrographs. It is obvious that, with decreasing pore diameter of the inorganic network, the surface area increases and the nanoparticle diameter decreases.

The diameter of the different TiO_2 nanoparticles for the different networks varies from hundreds of nanometers to less than 10 nm depending on the initial polymer gel template. The particles within a single network are not monodisperse, with higher polydispersities being observed for the structures produced from polymer gels with larger pore diameters. During calcining it is believed that there is some fusing of the individual particles. The use of both HRTEM and WAXS confirmed that these particles adopt either the anatase or rutile crystal phases by controlling the temperature of calcination. The HRTEM micrographs show the single-crystal nature and the *d* spacing of the individual particles. WAXS confirms that the total structure is made up of colloids in the same crystal phase (i.e., the crystal purity exceeds our detection limit).

A comparison of the surface area measurements given for both the polymer gel and the resulting titanium dioxide structure reveals another trend: For the larger pore systems, the polymer gel and titanium dioxide structure have similar surface areas; for the smaller pore systems, the titanium dioxide has a larger surface area than the polymer gel. This supports the concept outlined above that a system with finer pores is coated with a thinner layer, which transforms into a porous, weakly connected crystalline network (i.e., the two-dimensional nature of the coating layer is lost for finer pores).

Incorporation of Platinum Nanoparticles. SE1 and SE2 polymer gels were used to demonstrate the possibility of building more complicated structures by the incorporation of platinum colloids into the polymer gel and then the final TiO_2 network. The gels went from white to yellow because of the platinum salt penetrating within the polymer structure. Leakage of a small amount of the platinum salt from the polymer gel, during solvent exchange, indicates the equilibrium nature of the binding process between the platinum salt and the polymer. Sufficient platinum salt remained in the polymer during both the solvent exchange and alcohol refluxing processes for there to be a dispersion of particles in the polymer after reduction of the metal salt. Following hydrolysis and condensation of the titanium precursor, the gels maintained their yellow color. After calcination, the platinum-containing TiO_2 networks were slightly gray.

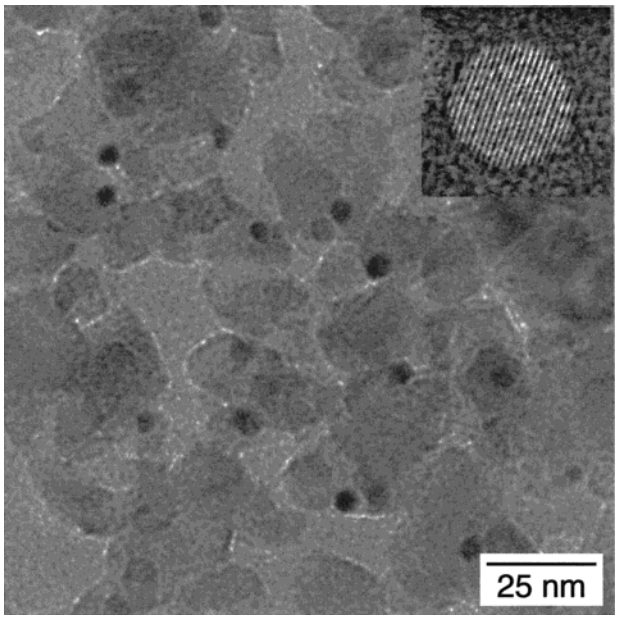

Figure 6. TEM micrograph of the TiO_2 network with homogeneously dispersed platinum nanoparticles. The inset shows the lattice planes of a platinum particle with lattice plane spacing of 0.222 nm.

Figure 6 shows the even distribution of the platinum particles in the TiO_2 network. The platinum colloids have a diameter of ca. 5−6 nm and are seen in the TEM micrograph as the more electron dense particles. The inset shows the HRTEM image of a single platinum particle, which has a *d* spacing of 0.222 nm. This image shows that the platinum particle is not oxidized, as might be expected after the calcination process. Again energy-dispersive X-ray analysis of this material did not detect carbon, indicating effective removal of the organic material during the calcination process.

Moreover, one can see the very good mutual dispersity and intense contact of the Pt and TiO_2 nanoparticles. This is significantly better than similar hybrid systems

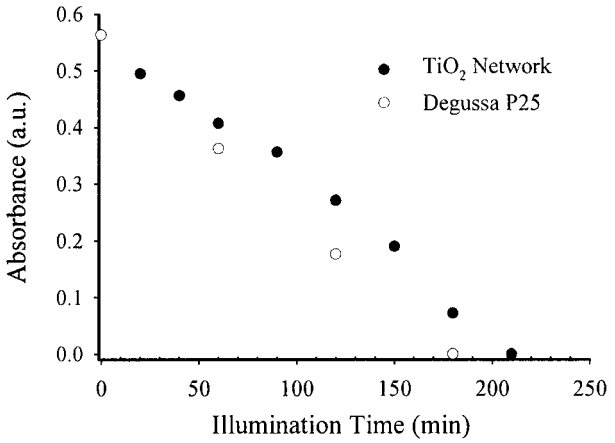

Figure 7. Salicylic acid absorbance monitored at a wavelength of 296 nm as a function of time in the presence of the porous TiO_2 network (filled circles) and Degussa P25 titania (circles). The samples were illuminated by a mercury lamp.

produced by postimpregnation techniques. The optimized structure is attributed to the structure-directing influence of the polymer and the dynamically hindered exchange processes at the gel surface.

Salicylic Acid Photodecomposition. For testing the photocatalytic activity of these structures, we used as a model case the decomposition of salicylic acid in an aqueous solution under air. The activity of pieces of the highly porous titanium dioxide network was compared with that of a Degussa P25 powder. Figure 7 shows the change in absorbance at a wavelength of 296 nm with time for the two samples. After the same illumination time, the decomposition of the organic material using the porous titanium dioxide structure is 75% of that obtained by the powdered Degussa P25. It should be pointed out that within the restrictions of this comparison, i.e., the difference in the applicable geometry of the catalysts—powder compared to network structure—the data are promising. The platinum-loaded titanium dioxide sample also decomposed the salicylic acid; however, leeching of platinum particles occurred, which was seen in the absorbance spectra for this sample.

Summary and Outlook. The production of TiO_2 structures using polymer gel templating procedures provides a means to develop highly porous and high surface area materials and is a valuable addition to other methods of templating used to form controlled structures. The ability to control the pore size, porosity, and network structure originates from the adaptability of the initial polymer gel template. A mechanism for the TiO_2 incorporation within the polymer gel structure is proposed. First, TiO_2 does not completely fill the structure but instead hydrolyzes and condenses, resulting in it coating the polymer framework. This is illustrated in Figure 8, where schematic representations of the polymer gel (a) and the polymer gel coated with amorphous titania (b) are shown. During heating, the initial framework is removed (c) because polymer pyrolysis and crystallization of the titania occur, thereby producing TiO_2 colloidal particles. The end result (d) is plating of the original gel, leaving a porous crystalline system with dimensions similar to those of the original polymer gel. It turned out that this porosity sensitively depends on the coupled properties "pore size" and "thickness of the coating layer", where smaller pores and thinner layers produce less cohesive crystalline layers.

The combination of high surface area and high porosity of the TiO_2 network is expected to enhance the wide and ever-growing range of applications for which titania is currently employed, such as environmental cleanup,[30] water and air purification,[31] and "self-cleaning" of ceramic tiles.[20] In the dye-sensitized solar cell application, an increase in the surface area and porosity of the titanium dioxide results in a higher degree of TiO_2—charge-transfer dye contact and therefore an increase in the photovoltaic efficiency of the material.[32] The photocatalytic properties of a more porous, higher surface area titanium dioxide will also be enhanced because of the increased number of reactive sites, simply because of more catalyst—reactant contact.

The incorporation of platinum within the TiO_2 network adds extra dimensions to this templating procedure. The ability to homogeneously distribute the nanoparticles within the inorganic material in this simple fashion opens many new possibilities. It can potentially be extended to other nanoparticles, such as semiconductor quantum dots with tailor-made band gaps. The concept of a multilayer coating with a directional gradient of optical and electronic properties potentially extends this approach to two-dimensional objects with two different sets of interfaces.

Our current projects involve production of such porous oxide layers in thin films,[33] the employment of such films to determine the photovoltaic and photocatalytic efficiencies, and an extension of this technique to other

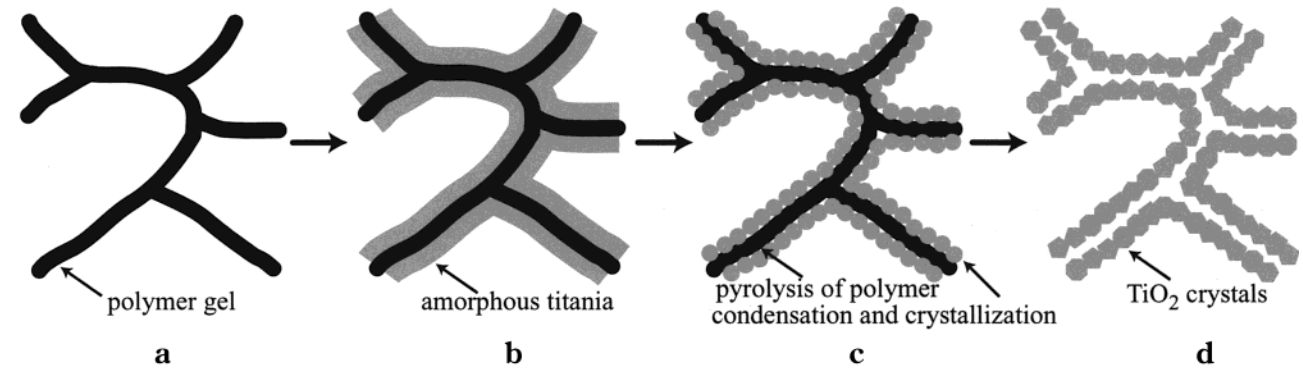

Figure 8. Schematic of polymer gel coating by titanium dioxide: (a) polymer gel, (b) incorporation of precursor, followed by hydrolysis; (c) drying and calcination; (d) the final network, which is a coating of the initial polymer gel.

metal oxide systems. The photodecomposition of salicylic acid using these porous structures already occurs at around 75% efficiency of Degussa P25 titanium dioxide. A more detailed study on the application of our materials is currently underway.

Acknowledgment. Rona Pitschke and Ulrike Bloeck are thanked for the ultramicrotoming and ion milling of the polymer and TiO_2 samples, and Ingrid Zenke is thanked for conducting the WAXS measurements. Degussa-Hüls is thanked for the titanium dioxide P25 sample.

CM001222Z

(30) Hoffmann, M. R.; Martin, S. T.; Choi, W.; Bahnemann, D. W. *Chem. Rev.* **1995**, *95*, 69−96.
(31) (a) Legrini, O.; Oliveros, E.; Braun, A. M. *Chem. Rev.* **1993**, *93*, 671−698. (b) Sauer, M. L.; Ollis, D. F. *J. Catal.* **1996**, *158*, 570−582.
(32) O'Regan, B.; Grätzel, M. *Nature* **1991**, *353*, 737−740.
(33) Caruso, R. A.; Schattka, J. H. *Adv. Mater.* **2000**, *12*, 1921−1923.